Fuel 324 (2022) 124761

Contents lists available at ScienceDirect

Fuel

journal homepage: www.elsevier.com/locate/fuel

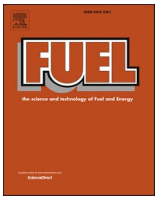

Combustion performance of low calorific gas enriched by oxygen and ozone

R. Paulauskas, R. Skvorčinskienė *, K. Zakarauskas, N. Striūgas

Laboratory of Combustion Processes, Lithuanian Energy Institute, Breslaujos str. 3, LT-44403, Lithuania

ARTICLE INFO

Keywords:
Low calorific gas
Plasma-produced ozone
Oxygen-enriched air
Combustion
Flame emission spectroscopy
Flame lift-off
NOx

ABSTRACT

Biomethane produced via anaerobic digestion or thermochemical process is one of alternatives, which could substitute fossil fuel and reduce carbon footprints. However, during biomethane preparation for end-users, the waste gas stream could be formed during biogas upgrade/methanation. As these gases consists of few to 30 vol% of methane in CO_2, the waste gas stream should be utilized instead of emission to atmosphere. Aside, to achieve clean and stable combustion of such gases, innovative methods are required as high concentrations of CO_2 causes the decreased flame temperature and burning velocity.

This study concerns the low calorific gas combustion enhancement by oxygen enriched air and plasma-produced ozone. The ozone-assisted combustion was investigated by burning various composition waste gases (30–15 vol% of CH_4 in CO_2) in a low swirl burner under different oxygen enrichment levels, from 28 to 80 vol%. It was determined that the combustion enhancement by ozone is related to methane concentration in the mixture and to oxygen enrichment level. Moreover, at lower oxygen enrichment levels, the combustion enhancement by the ozone addition was more pronouncing than at higher oxygen enrichment levels. The flame lift-off was reduced by 0.9–25.9% due to the ozone addition and the flame stability improved, but NOx emissions increased by 2–10 ppm compared to cases without O_3 addition. Considering the combustion efficiency in terms of flame lift-off height, NOx and CO emissions, the ozone-assisted combustion of WG25 and WG20 was the most efficient under oxygen enrichment of 40 vol% compared to other cases.

1. Introduction

Over the last century ongoing CO_2-induced climate change brought government and public attention on environmental concerns. For this reason, the EU issued The European Green Deal which aims to fully decarbonize energy, industry and transport sectors by 2050. Moreover, it is foreseen to reduce the GHG emissions at least 50% by 2030 and boost the share of renewable energy sources as well [1]. In the view of ambitious plans, biomethane is a valuable renewable energy resource that can be an alternative solution for the world's insatiable energy demands and at the same time help in reducing bio-waste and greenhouse gas emissions [2,3]. Also, biomethane could substitute fossil fuels for heat, electricity production and co-generation, vehicle fuel, etc. The biomethane is obtainable from biogas via anaerobic digestion [4,5]. Biogas used as a high-value product should be upgraded and various impurities like carbon dioxide, nitrogen, oxygen separated [6]. In recent years, membrane separation technologies have been used to upgrade biogas for simplicity [7]. This technology is cost-effective, but the deficiency of it is a considerably low methane yield due to imperfect separation and the biogas could be upgraded only up to 92 vol% CH_4 in one-stage mode. In some cases, the biogas purification are improved by increasing the number of membrane modules then the part of permitted gas could be reached up to 96 vol% of methane. However, during optimal conditions of biogas purification, the waste gas stream could be formed, which contains from 15 to 30% of CH_4 in CO_2. These gases should be utilized on-site due to carbon footprint, but a considerably high CO_2 concentration and low calorific value (7–11 MJ/m^3) results in unstable combustion of waste gases.

During the last decade, plasma-assisted combustion has gained a lot of interest as an innovative method to enhance the combustion process. Various types of plasmas like a dielectric barrier discharge plasma [8–10], a repetitive pulsed plasma [11,12], a gliding arc plasma [13] and a laser-induced plasma [14] were used to increase lean burn flame stability, enhance low temperature fuel oxidation, ignition, combustion efficiency under a wide range of conditions. For example, the use of dielectric barrier discharge improved the flame stability of jet flames and flame speed was enhanced by about 125% [15]. Other researches revealed that the combustion enhancement by nanosecond repetitively-

* Corresponding author.
E-mail address: Raminta.Skvorcinskiene@lei.lt (R. Skvorčinskienė).

https://doi.org/10.1016/j.fuel.2022.124761
Received 2 December 2021; Received in revised form 30 April 2022; Accepted 2 June 2022
Available online 8 June 2022

pulsed plasma discharges not only improves the flame stability, but also extends the flammability limit and increases the flame temperature [16–18]. Based on [16] the flammability limit of propane was extended from $\phi = 0.4$ to 0.11 at 30 kHz repetition rate, while for methane it was extended only from $\phi = 0.6$ to 0.53 increasing the repetition rate from 10 kHz to 50 kHz [18]. But according to [17] the methane flame speed was increased up to 100% due to increased flame temperature by nano second repetitive plasma discharges. Sagás et al. [19] performed plasma-assisted combustion of methane/air premix at the fuel-rich conditions using gliding arc discharges. The results showed the upper limit of flammability increased from $\phi = 1.3$ to 2.2 at an applied plasma power of 390 W, but additional NO formation due to plasma discharges in air was observed by flame emission spectroscopy. The increased formations of prompt and thermal NOx resulting in increased emissions compared to the case without plasma were also indicated by other works [20–22]. For example, Kim et al. [23] determined that NOx emissions increase from 5 to 20 ppm with increasing fuel to air ratio ϕ from 0.5 to 0.65 during plasma assisted combustion. In this case the addition of plasma-produced ozone could mitigate the issue of plasma-assisted combustion and enhance the flame stability and flammability. According to [24], ozone addition of 3% increases the flame velocity of ethylene/methane flames. Meanwhile, the addition of small amounts of ethylene (10–20 vol%) to methane led to almost the same relative increase in flame velocity under the addition of ozone as pure ethylene. Other work [25] indicates that the O_3 addition of 14000 ppm increases the flammability limit and laminar flame speed of the $H_2/CO/O_2$ mixture. Authors determined that the O_3 interaction with fuel causes a group of chain branching reactions resulting in production of active radicals (e.g., O, OH, etc.). Similar results were also determined during ozone-assisted methane combustion [26]. The ozone addition increased the laminar flame speed and laminar burning velocity changing fuel to air ratio ϕ from 0.6 to 1.2, but in fuel-rich case, the flame instability was intensified. Moreover, the ozone addition showed greater effect on flame speed improvement at lean-fuel conditions.

According to reviewed works, ozone has long lifetime compared to other plasma produced species/radicals, which influence the combustion process and an implementation of this method does not require major upgrades compared to plasma-coupled flame. Though, to prevent the undesired plasma by-products like NOx [27], a supply of pure oxygen for ozone production should be ensured. Considering that, the ozone addition could be coupled with oxygen enrichment as the supply of oxygen enriched air shows promising results on combustion enhancement [2829]. For example, oxygen enrichment between 21 vol% and 30 vol% results in improved CH_4/CO_2 flame stability and efficiency, but the increased oxygen enrichment led to higher flame temperature, which in turn resulted in increased NOx emissions [30]. Study on biogas flame stability improvement in a premixed burner at oxygen enrichment levels of 24 vol%, 28 vol% and 31 vol% [29] revealed that the most efficient combustion process in terms of flame stability and low pollutant emissions is achieved at oxygen enrichment level 24%, while at higher O_2 enrichment levels, flame stability started to decrease. Unstable combustion was observed supplying the oxygen-enriched air by 31 vol%. Similar findings were provided by [31]. Stable oxy-fuel combustion of methane was achieved when oxygen mole fraction in the oxidizer was below 0.5, but at higher values (from 0.6 to 1.0), the combustion process became unstable. Though, opposite results were observed during biogas combustion with different composition oxidizers in a swirl combustor [32]. Oxy-fuel combustion (O_2-100 vol%) led to increased flame temperature near fuel inlet region due to intensified fuel oxidation, while using a diluted oxidizer (O_2-40%/CO_2-60%), the flame temperature decreased and the combustion characteristic were similar to the case with air.

Considering that the biomethane production and usage rates are increasing, the combination of ozone addition and oxygen enrichment could be a cheap and attractive solution to ensure stable and clean combustion of waste gases. Moreover, the implementation of this method does not require changes in a burner configuration or new designs as in the case of plasma-assisted combustion. Besides, literature review shows that number of works related to ozone-assisted combustion is very limited and there is a need of the knowledge of ozone-assisted LCV combustion. For these reasons, this work analyses the combustion enhancement of various waste gas mixtures by oxygen and ozone addition. Flame characteristics under oxygen and ozone enrichment were determined using the flame emission spectroscopy method for registering chemiluminescent radical species OH*, CH* and C_2*. Based on acquired OH* emission intensity, the flammability limits of waste gas mixtures were determined. In addition, post combustion products during combustion under oxygen and ozone enrichments were measured and the combustion efficiency in terms of CO emissions was estimated based on the flame lift-off heights.

2. Experimental methodology

2.1. Experimental combustion rig

The experiments were performed in a special experimental rig, which allows to combust various gases with different calorific value and test different combustion enrichment methods [33,34]. To investigate waste gas combustion under oxygen and ozone enrichment, a DBD plasma reactor was installed (Fig. 1).

The combustion process was performed in a low swirl burner, which is suitable for combustion process at very lean-fuel conditions. The burner consists of three main parts: a burner surface, a swirler and a nozzle outlet of quartz glass. The swirler of 20 mm outer diameter and 11.6 mm inner diameter has fifteen straight vanes fixed at angle of 53°. The vanes are arranged around a centreline channel. It ensures that most of the flow pass through the vanes and only around one-third of the flow goes through a central perforated plate. The swirl number corresponds to value of SN = 1.04 based on geometric parameters of the burner. The burner was covered with the clean quartz glass tube of 73 cm height and 13 cm diameter, which ensured a required light transmittance (>90%) for the flame spectroscopy. The tube was used as a combustion chamber and a shield to prevent ambient air suction as well. A flue gas sampling probe was installed inside the chamber at a distance of 60 cm from the burner surface for sampling. A Testo 350XL analyser was connected to the sampling probe to measure emissions of NOx, CO, and CO_2 in flue gas (Fig. 1). An intensified charge coupled device (ICCD) camera Andor iStar DH734 with lenses was used to capture a spatial distribution of the excited OH*, C_2* and CH* radicals from the flame.

2.2. Gas mixture preparation and procedure

For the experiments, waste gases with low calorific value were simulated by preparing various mixtures of CH_4 and CO_2 (carbon dioxide). Methane concentration was changed from 30 vol% to 15 vol% in CO_2. As the combustion of the waste gases was not possible supplying an air composition oxidizer due to flame blowoff, the oxidizer was enriched by oxygen at different proportions (see Table 1). To avoid, NO formation by plasma, nitrogen and oxygen was supplied separately and the ozone (about 6000 ppm) was produced by supplying oxygen through the co-axial DBD plasma reactor. Although, all gases (CH_4, CO_2, O_2 and N_2) were supplied by separate inlets and a precise preparation of a premix was ensured by controlling each flow of gases with mass flow controllers BROOKS. This allowed to change the flow rate of the premix to keep a constant capacity of burner's thermal power (2 kW) during combustion. The combustion process was performed at lean-fuel conditions and the fuel-air equivalence ratio (ϕ) was changed from 0.63 to 1.0 during the experiments. The fuel-air equivalence ratio (ϕ) was calculated as follows:

$$\phi = \frac{Q_{CH4}/Q_{Oxidizer}}{(Q_{CH4}/Q_{Oxidizer})_{st}} \quad (1)$$

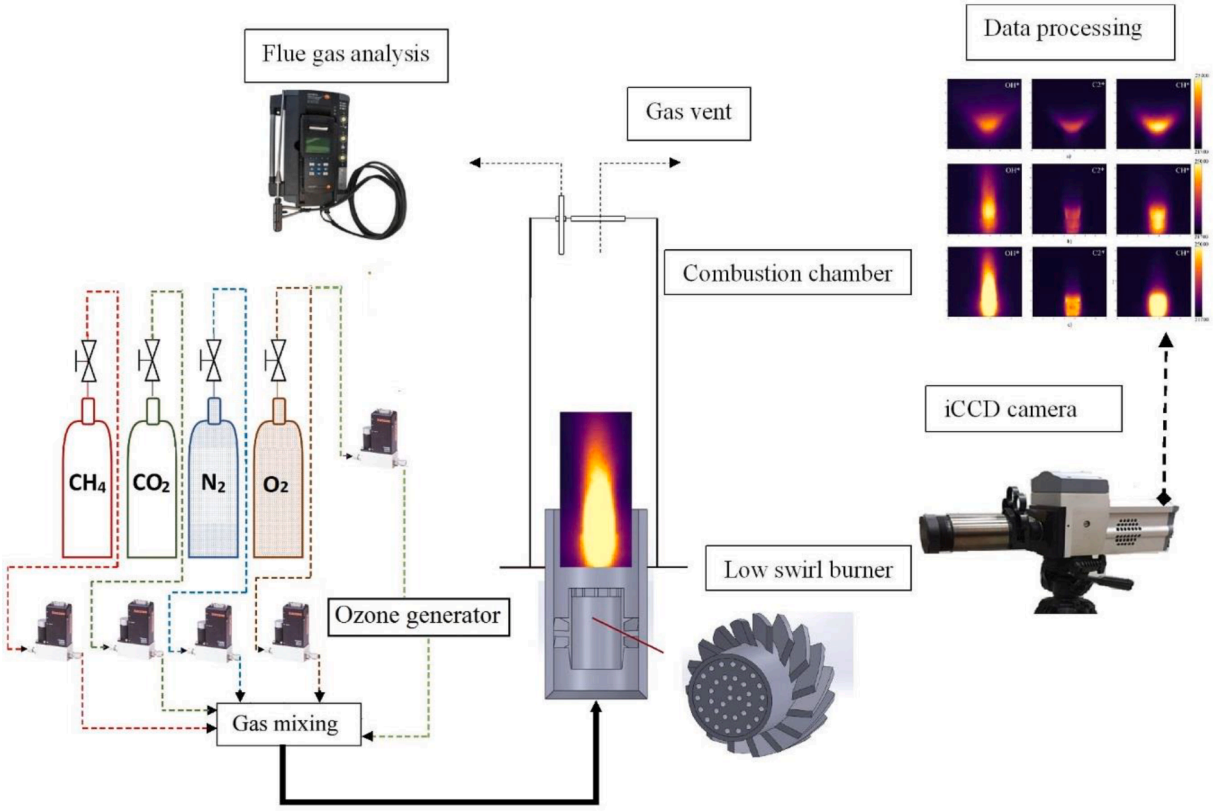

Fig. 1. Schematic diagram of the experimental rig for investigation of waste gas combustion under oxygen and ozone enrichment.

Table 1
Composition of used gases.

Gases	Composition	Oxidizer, O_2 in N_2	Fuel-air equivalence ratio ϕ
WG30	CH_4-30%/CO_2-70%	28% 30%	0.91, 0.83, 0.77, 0.71, 0.67 0.91, 0.83, 0.77, 0.71, 0.67, 0.63
WG25	CH_4-25%/CO_2-75%	30% 40%	0.83, 0.77, 0.71 1.0, 0.91, 0.83, 0.77, 0.71, 0.67, 0.63
WG20	CH_4-20%/CO_2-80%	35 % 40% 60%	0.77, 0.71 0.83, 0.77, 0.71, 0.67, 0.63 1.0, 0.91, 0.83, 0.77, 0.71, 0.67, 0.63
WG15	CH_4-15%/CO_2-85%	55% 60% 80%	0.77, 0.714, 0.67, 0.63 0.83, 0.77, 0.71, 0.67, 0.63 0.83, 0.77, 0.71, 0.67, 0.63

where, Q represents the actual volumetric flow of CH_4 and air, and suffix *st* stands for the stoichiometric volumetric flow conditions.

2.3. Flame emission spectroscopy

The combustion process was observed using an optical system for analysis of spatial distribution of the excited species OH* (310 nm), CH* (387 nm) and C_2* (514 nm) from the flame at atmospheric pressure. The flame images were captured using an ICCD (Intensified Charge Coupled Device) camera (Andor iStar DH734i-18-UE3) sensitive for 200–800 nm wavelength light with bandpass filters mounted directly in front of the camera objective (OH*, CH*, C_2*). The camera consists of the photocathode with a diameter of 18 mm and the pixel size is 13 μm. The Equivalent Background Illuminance is lower than 0.2 e−/pix/sec. The camera was mounted at a distance of 70 cm from the burner and focused on the flame in such a way that the flame fits the image frame entirely. The ANDOR SOLIS software was used to operate the camera, save acquired emission intensities and to convert raw data to flame images. Also collected data was processed using the open-source programming software Python 3.6 [50] and each horizontal line of the pixel intensity values in the frame was averaged, thereby producing the averaged distribution of chemiluminescence intensity along the flame axis, representing relative emission intensities of chemiluminescent species along the burner axis. Further, the highest intensity value along the burner axis was attributed to a flame attachment position.

To reduce the effect of flame instability for each flame condition and each filter, and to compensate for light intensity loss by the quartz glass tube (transparency of >90%), a single flame image was achieved by averaging 30 image acquisitions each with an exposure time of 0.04 s and the accumulation time was 36.18 s. The resulting flame image resolution was 6.6 pixels per millimetre. The uncertainty of the overall accuracy of the equipment was assessed. Moreover, the other uncertainty from the mean values was also estimated. The experimental equipment was calibrated by the manufacturer. Operating parameters and deviations are also described in the manufacturer's manual. Uncertainty in the operation of the device was determined by repeated series of experiments and standard deviation as the overall accuracy of the measurement was calculated. According to the calculations, it can be stated that it has never exceeded >2% of the absolute value measured at each wavelength.

3. Results and discussions

3.1. Flammability of waste gases

Firstly, the waste gas flammability under oxygen enrichment was investigated by changing the O_2 enrichment. The flammability map was prepared based a single accumulated image of OH* emissions from the flame (Fig. 2). It was determined that the lowest O_2 enrichment level for stable combustion of WG30 is 28 vol% and a conical flame is formed. An increase of O_2 concentration in air to 30 vol% intensified fuel oxidation and resulted in higher OH* emission intensities. It is well known that the oxygen addition enhances the combustion process and OH* formation rates increase based on this reaction: $CH + O_2 \rightarrow OH^* + CO$ [35]. Though, a higher O_2 enrichment level caused a change of the flame shape from conical to column one indicating that the flame approached close.

to the flashback limit. At higher oxygen enrichment levels, an increasing O_2 part in air reduces the mixture injection velocity and a decrease of axial velocity leads to flame flashback or vice versa. The stable combustion process of WG25 mixture was achieved at oxygen enrichment levels of 30 and 40 vol%. At higher or lower O_2 enrichment levels flame flashback or flame blowoff occurred, respectively (Fig. 2). In case of WG20, the combustion process was able supplying oxygen enriched air by 35–60 vol% of O_2, while the combustion of WG15 mixture was achieved only supplying air enriched by 55–80 vol% of O_2. Using the determined values of oxygen enrichment level, the waste gas combustion was investigated supplying ozone (~6000 ppm) produced via the DBD reactor. The obtained images of ozone-assisted waste gas flame are compared to ones without the ozone addition in Fig. 2. According to flame images, the ozone addition leads to the increased OH* emission intensity and change of the flame shape, which is close to the blowoff limit. It is assumed that the fuel oxidation becomes more intensive due to ozone addition leading to increased OH formation, which in turn is closely related to the flame temperature increase [36].

3.2. Analysis of oxygen-enriched and ozone-assisted flames

In order to understand how the oxygen enrichment and ozone addition (~6000 ppm) affect the chemiluminescence spatial intensity of species such as OH*, CH*, and C_2* from waste gas flames, the average emission intensities of these radicals were estimated at the different oxygen enrichment levels and fuel-air equivalence ratios ϕ. The evaluated graphs are presented in Fig. 3. During combustion of WG30, it was determined that the OH*, C_2* and CH* emission intensities increase changing oxygen enrichment level from 28 to 30 vol%. This tendency was also determined with other WG mixtures, but due to lower calorific value and negative CO_2 influence, the emission intensities were lower at similar oxygen enrichment levels. In the case of ozone addition, the increase in registered radical emission intensities was determined at both oxygen enrichment levels (28 and 30 vol%). However, at oxygen enrichment level of 28 vol%, the increase was insignificant at leaner fuel conditions and average intensity of OH*, C_2* and CH* emissions increased by 5.6%, 1.6% and 4.3%, respectively, compared to the case without the ozone addition only at $\phi = 0.91$ (Fig. 3). A bit different results were obtained at oxygen enrichment level of 30 vol%. Due to addition of ozone, the intensities of OH* and CH* emissions increased from 2.1 to 2.6% and the intensity of C_2* emission increased from 1.4 to 1.8% changing ϕ values from 0.63 to 0.91 compared to the case without the ozone addition. These trends also corresponded to the changes in flame lift-off positions and a decrease in emission intensities of registered radicals (from $\phi = 0.83$ to 0.91) coincide with the flame shift to the blow-off limits (see Fig. 3 and Fig. 4). This was also determined with further waste gas mixtures. According to [37], ozone reacts with O, H and OH radicals by reactions ($O_3 + H = O_2 + OH$), ($O_3 + H = O + HO_2$),

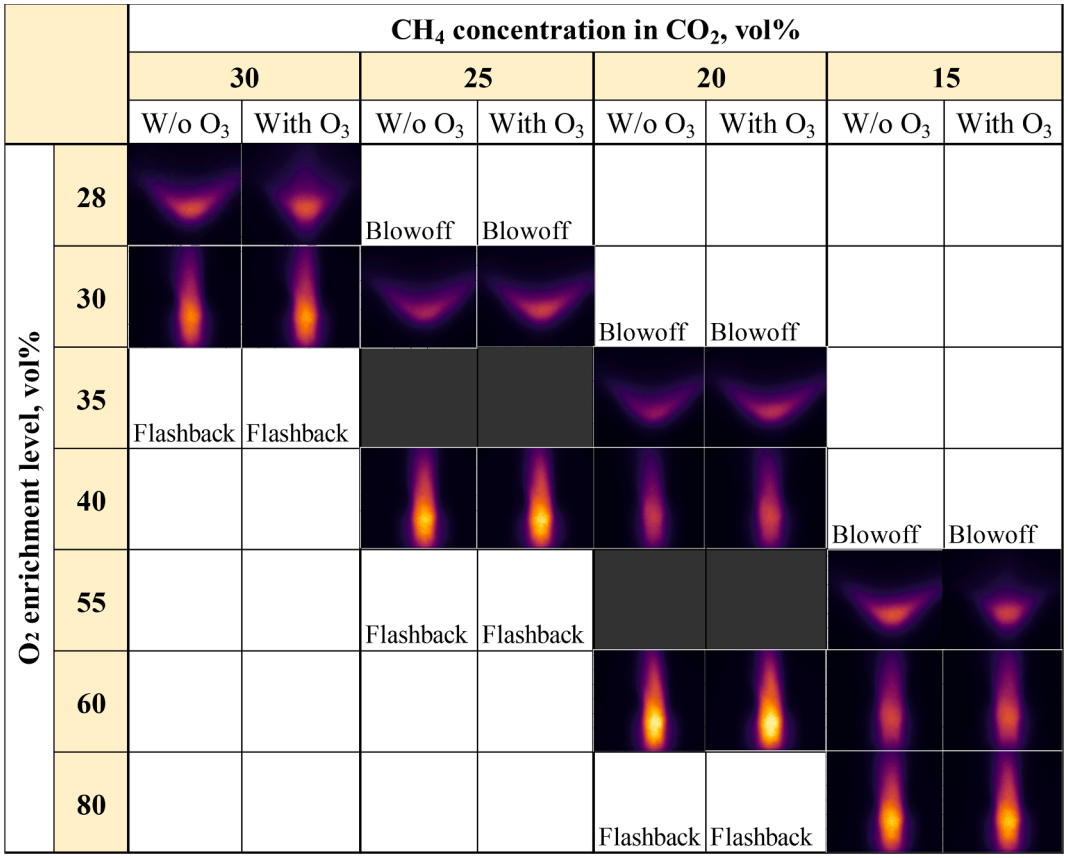

Fig. 2. Flammability map of waste gases under oxygen and ozone enriched conditions.

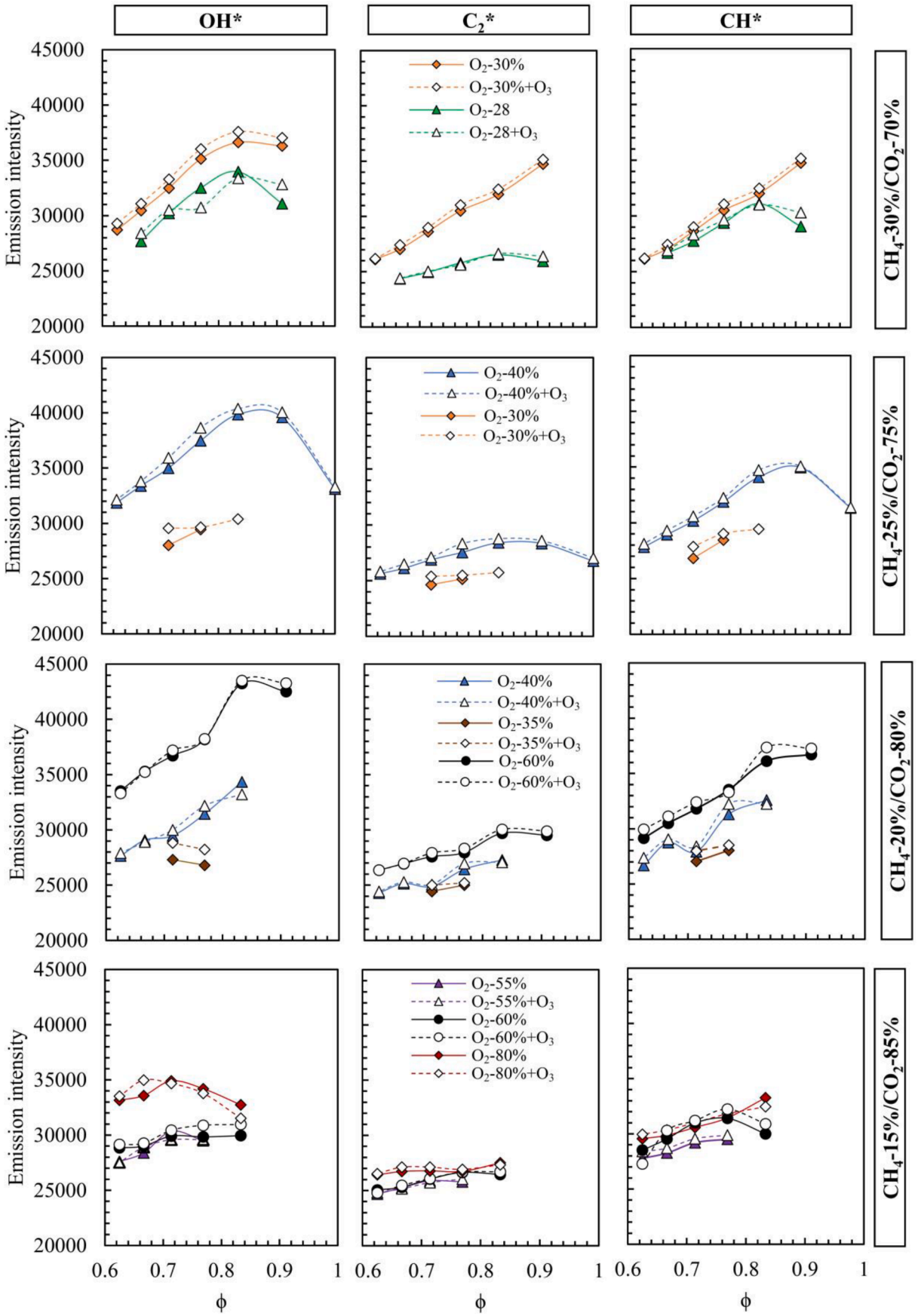

Fig. 3. Average emission intensities of OH*, C_2* and CH* from different waste gas mixtures under oxygen and ozone enriched conditions versus fuel-air equivalence ratio ϕ.

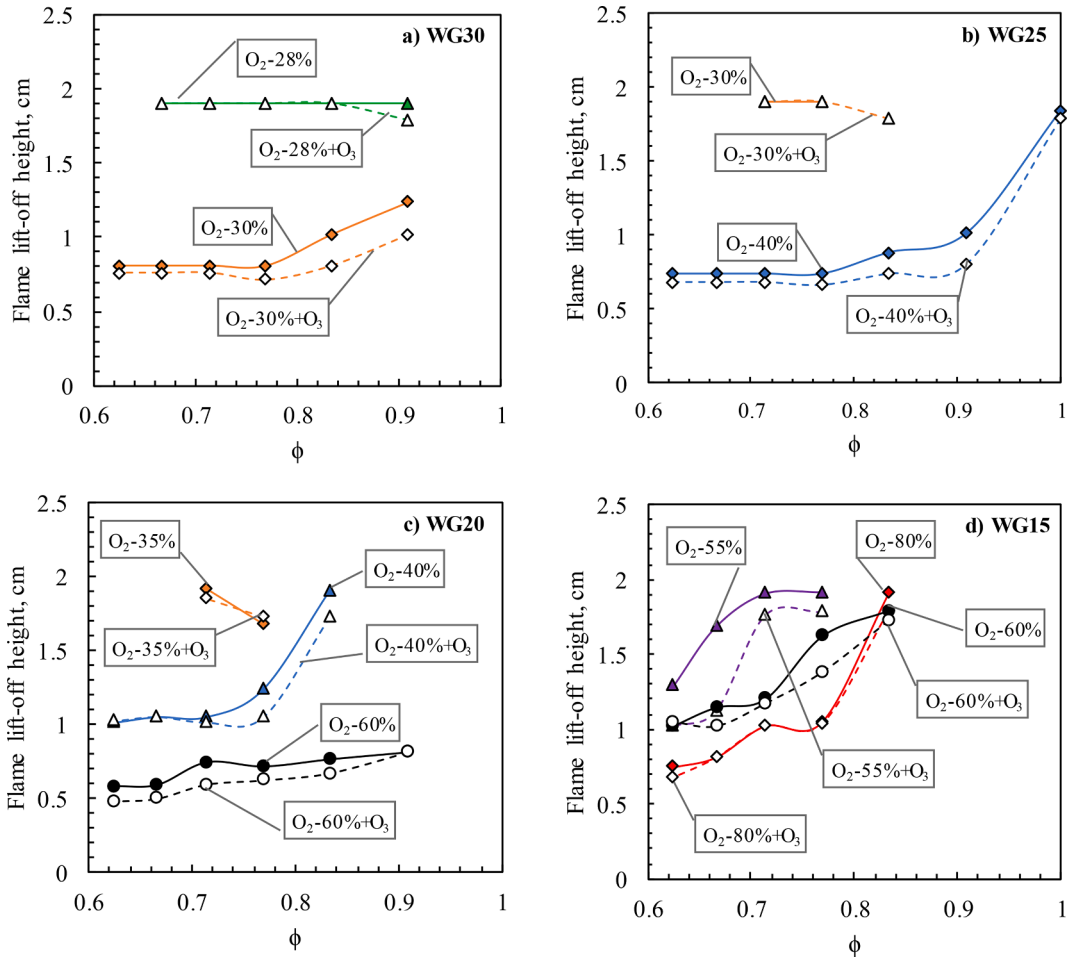

Fig. 4. Vertical flame position during combustion of waste gases under oxygen enrichment without and with ozone addition versus ϕ.

($O_3 + OH = O_2 + HO_2$) and ($O_3 + O = O_2 + O_2$) [38] causing more intensive formation of intermediate species like HO_2, H_2O_2, and CH_2O whose enhances the burning velocity through chain-branching reactions and the flame stability is improved. The combustion of WG25 with O_2 enriched air by 30 vol% resulted to lower emission intensities of registered radicals compared to the case of WG30 under identical conditions and narrow flammability of this mixture. Though, the ozone addition resulted in increased emission intensities of OH*, C_2* and CH* by about 5.5%, 3% and by 3.9% and extended flammability range up to $\phi = 0.83$ (Fig. 3). At O_2 enrichment level of 40 vol% the emission intensities of these radicals increased up to 30% compared to the case of O_2 enrichment level of 30 vol% and the combustion process of WG25 was achieved at all tested ϕ values. Considered the ozone addition, emission intensities of OH*, C_2* and CH* increased only around by 3.2%, 2.8% and by 1.4% (Fig. 3), but it led to decreased flame lift-off height (Fig. 4b). It was determined that the ozone effect on radical emission intensities was less pronounced decreasing CH_4 in the mixture and increasing oxygen enrichment level. For example, in the case of WG20 under oxygen enrichment of 60 vol%, the emissions intensity of registered radicals increased only up to few percent, while at lower oxygen enrichment ($O_2 = 40$ vol%) the emissions intensity of OH*, C_2* and CH* increased by approximately 2.4%, 2% and by 3% at tested O_2 enrichment levels. The highest ozone effect was determined at the lowest oxygen enrichment level ($O_2 = 35$ vol%), but at this enrichment point the flame was close to the blow-off limit. Analysis of the obtained data reveals that the increase in emission intensities of registered radicals due to the ozone addition are lower at higher oxygen enrichment levels. This trend was opposite analysing the flame lift-off changes as with the increasing oxygen enrichment level, the ozone effect led to more attached flame to the burner nozzle (see Fig. 4c). Considering that similar trend was also observed with WG15 mixture, the decreased ozone effect with the increased oxygen enrichment level could be related to the decreased methane content in the mixture. According to [39], the increased CO_2/decreased CH_4 content in the mixture deaccelerate the chain branching reaction as fuel molecules are less to interact with ozone and reduces rates of reactions R1 ($O + H + M \rightarrow OH^* + M$) and R2 ($CH + O_2 \rightarrow OH^* + CO$). Besides, during O_3 decomposition formed O could be consumed for C_2* excitation reaction R3 ($C_3 + O \rightarrow C_2^* + CO$) [40]. Considered the obtained results, the ozone enhanced species could be also consumed in the reaction R4 ($C_2 + OH \rightarrow CH^* + CO$) which is decelerated due to increased oxygen enrichment level and leads to decreased C_2* emission intensity, but increased CH* one [41].

For better understanding how the flame position is influenced by oxygen enrichment and the ozone addition effect on the flame stability, the flame lift-off heights were estimated from registered OH* emission intensities. From previous studies [10,33,34], it was determined that the average value of maximum intensities could be attributed to the flame position, which changes depending on combustion conditions. Decreasing CO_2 concentration in waste gases or increasing O_2 enrichment level in the oxidizer results in increased flame stability and the maximum value of OH* emission intensity moves closer to the burner exit or vice versa. The estimated flame lift-off heights are presented in Fig. 3. During combustion of WG30 mixture with oxygen enriched air by 28 vol%, the flame lift-off height was around 1.9 cm from the burner nozzle at all tested ϕ values. Considering the determined flammability

limits (Fig. 2), the flame lift-off height of 2 cm can be assumed as a threshold above the flame approaches to blowoff. The increased oxygen enrichment level from 28 vol% to 30 vol% led to reduced flame lift-off by 60% and increased flame stability. Besides, the ozone addition showed more intensive improvement on the WG30 flame stability at higher oxygen enrichment level (O_2-30 vol%). The flame lift-off was reduced by 6% only at $\phi = 0.91$ under oxygen enriched conditions (O_2-28 vol%), while supplying O_2 enriched air by 30 vol%, the flame lift-off was reduced from 6.3 to 25.9% changing fuel–air equivalence ratio ϕ from 0.63 to 0.91 (Fig. 3a). Besides, a higher effect of ozone was determined for ϕ values, at which the WG30 flame lift-off height started to increase. Similar results were obtained during combustion of WG25 mixture supplying oxygen-enriched air by 30 and 40 vol%. At lower oxygen enrichment level (30 vol%), the combustion process of WG25 was only achieved at $\phi = 0.71$–0.77 and the determined flame lift-off heights indicated that the flame is close to blow-off limit (Fig. 3b). The ozone addition extended the flammability of WG25 and the combustion process was achieved at $\phi = 0.83$, but no effect was observed on the flame lift-off reduction (Fig. 3b). In the case of oxygen enrichment by 40 vol%, the combustion process was achieved at all tested ϕ points, but increasing ϕ from 0.77, the flame shifted up and at $\phi = 1.0$, the flame was close to the blow-off limit considering that the estimated lift-off height was 1.7 cm from the burner nozzle. Analyzing ozone addition, it was determined that the flame lift-off height was reduced by 8.3 to 25.9% increasing ϕ from 0.63 to 0.91 (Fig. 3b). Meanwhile, at $\phi = 1.0$, the flame lift-off was reduced only by 3.2% compared to the case without ozone addition. Considering that this tendency was also observed in the case of WG30, it could be assumed that ozone has weaker effect in terms of flame lift-off reduction on the flames near the blow-off limit (Fig. 3). The similar trend was determined with further mixtures as well. For instance, during combustion of WG20 under the oxygen enrichment level of 35 vol%, the determined flame position was located near the blow-off limit and the flame-lift off was only reduced by 1.06% compared to the case without ozone addition. The increasing oxygen enrichment level by 5 vol% ensured stable combustion of WG20 mixture. According to flame lift-off heights, the flame was attached at around 1 cm from the burner nozzle changing ϕ from 0.63 to 0.71. However, approaching to richer combustion conditions ($\phi \geq 0.83$), the flame position shifted up, till 1.9 cm from the burner nozzle (Fig. 4c). As in the case of WG30, the most notable effect of ozone was determined for ϕ values, at which the shift of flame occurred. The flame lift-off was reduced from 3.8 to 10% changing ϕ from 0.63 to 0.83 compared to the case without ozone addition. A bit different results were obtained under the oxygen enrichment level of 60 vol%. Based to the flame lift-off heights (Fig. 4c), the WG20 flame was attached closer to the burner nozzle and a notable increase in the flame lift-off was not observed changing ϕ from 0.63 to 0.91 compared to the case with lower enrichment level. Regarding to the flammability ranges (Fig. 2), it was determined that the WG20 flame under O_2 enrichment of 60 vol% is close to the flashback limit as the further increase of oxygen enrichment by few % led to flame flashback. Considering this, it was assumed that the flame lift-off height of 0.5 cm is a threshold indicating that the flame flashback limit is reached. Due to ozone addition, the flame lift-off height was reduced from 19 to 13.3% changing ϕ from 0.63 to 0.83 compared to the cases without ozone and the flame position shifted down (Fig. 4c). Moreover, it was determined that at higher oxygen enrichment level, the ozone effect is greater at leaner combustion conditions. The higher enhancement effect of ozone at lean-fuel conditions was also observed in other works. Wang et al. [37] determined that the ozone addition of 7000 ppm leads to increased burning velocity by 16% at lean-fuel conditions, while at rich-fuel conditions it increased only by 9%. Similar findings were also presented in [26]. Authors noted that the burning velocity increases by 19.7% at lean-fuel conditions due the ozone addition.

The described tendency was also determined in the case of WG15 combustion, but at lower oxygen enrichment levels (55 vol% and 60 vol %). It could be related to lower calorific value of the mixture and high content of CO_2 comparing to WG20 one as at oxygen enrichment level of 55 vol%, the WG15 flame was lifted and increasing ϕ it approached to the blowoff limit (Fig. 4d). Moreover, the combustion enhancement by ozone was more pronouncing than at higher oxygen enrichment levels. For instance, the flame lift-off height was reduced from 22.1% to 6.9 % changing ϕ from 0.63 to 0.77 compared to the case without ozone addition. An increased oxygen enrichment level by 5 vol% resulted in improved flame stability as the flame approached closer to the burner exit and the flammability range extended up to 0.83. Though, the flame lift-off height was reduced only from 10.8% to 3.7 changing ϕ from 0.66 to 0.83 due to the ozone addition. Moreover, at the oxygen enrichment level of 80 vol%, the ozone addition showed insignificant effect on the flame lift-off reduction (up to 1%), even though this oxygen enrichment level led to more stable flame as the flame moved closer to the burner exit (Fig. 4d). Considering the obtained results, it could be assumed that the combustion enhancement by ozone is closely related to calorific value in terms of methane concentration in the mixture and depends on the flame position as the highest effect of ozone was observed at combustion conditions between blowoff and flashback limits. To determine how the flame position and ozone addition correlates to waste gas combustion performance at different oxygen enrichment levels, the distribution of CO emissions versus the flame lift-off heights are discussed in next section.

3.3. Ozone influence on combustion performance and pollutant emissions

The combustion efficiency under oxygen and ozone enrichment was evaluated by measuring CO and NOx emissions during the combustion of waste gases. According to the directive of the 2015/2193/EU on pollutant (CO, NOx) emission limits [42], the new medium combustion plants have not to exceed 200 mg/m^3 of NOx and CO is not limited burning gaseous fuels other than natural gas. These limits were not exceeded performing the combustion of various waste gases under oxygen and ozone enrichment. It was determined that the NOx emissions were not higher than 45 ppm (110 mg/m^3) under oxygen enriched conditions (Fig. 6). Moreover, the determined CO emissions show a close relation with the flame lift-off (Fig. 5), but this trend has some exceptions related to oxygen enrichment level. For instance, in the case of WG30, CO emissions increased from 63 to 7595 ppm changing ϕ from 0.67 to 0.91, but the flame was lifted at all tested ϕ values close to the flame blow-off limit due to low oxygen enrichment level (28 vol%) (Fig. 5a). Analysing NOx emissions, it was determined that changing ϕ from 0.67 to 0.91, the NOx emissions increased from 5 to 16 ppm. The ozone addition showed insignificant effect of the flame lift-off reduction, but intensified fuel oxidation led to decreased CO emissions by 32–37 ppm and by 645 ppm at $\phi = 0.67$–83 and at $\phi = 0.91$, respectively. Meanwhile, NOx emissions increased by 5–10 ppm at $\phi = 0.67$–83, but no effect was observed at $\phi = 0.91$ (see Fig. 6a). All this indicates that the addition of O_3 leads to increased flame temperature. Besides, according to [38], the direct reaction of ozone with NO during combustion is hardly possible as ozone recombines at high temperatures. Moreover, few studies [43,44] show that the increment in NO is related to the increased flame temperature via the enhanced chain branching reaction. At higher oxygen enrichment level (30 vol%), it was determined that with occurrence of incomplete combustion of waste gases, CO emissions increase, and the flame is lifted and vice versa. The efficient combustion of WG30 was achieved in range of $\phi = 0.71$–0.83 as the CO emissions were 54–119 ppm and the flame was in the middle of stable combustion region (see Fig. 5a). Moreover, NOx emissions were in range of 37–36 ppm at these ϕ values above (Fig. 6a). The combustion enhancement by ozone led to the decreased CO emissions and flame lift-off height, indicating improved efficiency and stability of the combustion process. The addition of ozone reduced CO emissions by 10–43 ppm and also NOx emissions by 3 ppm at ϕ values mentioned above (Fig. 5a). Besides, significant effect of ozone was determined at leaner combustion ϕ

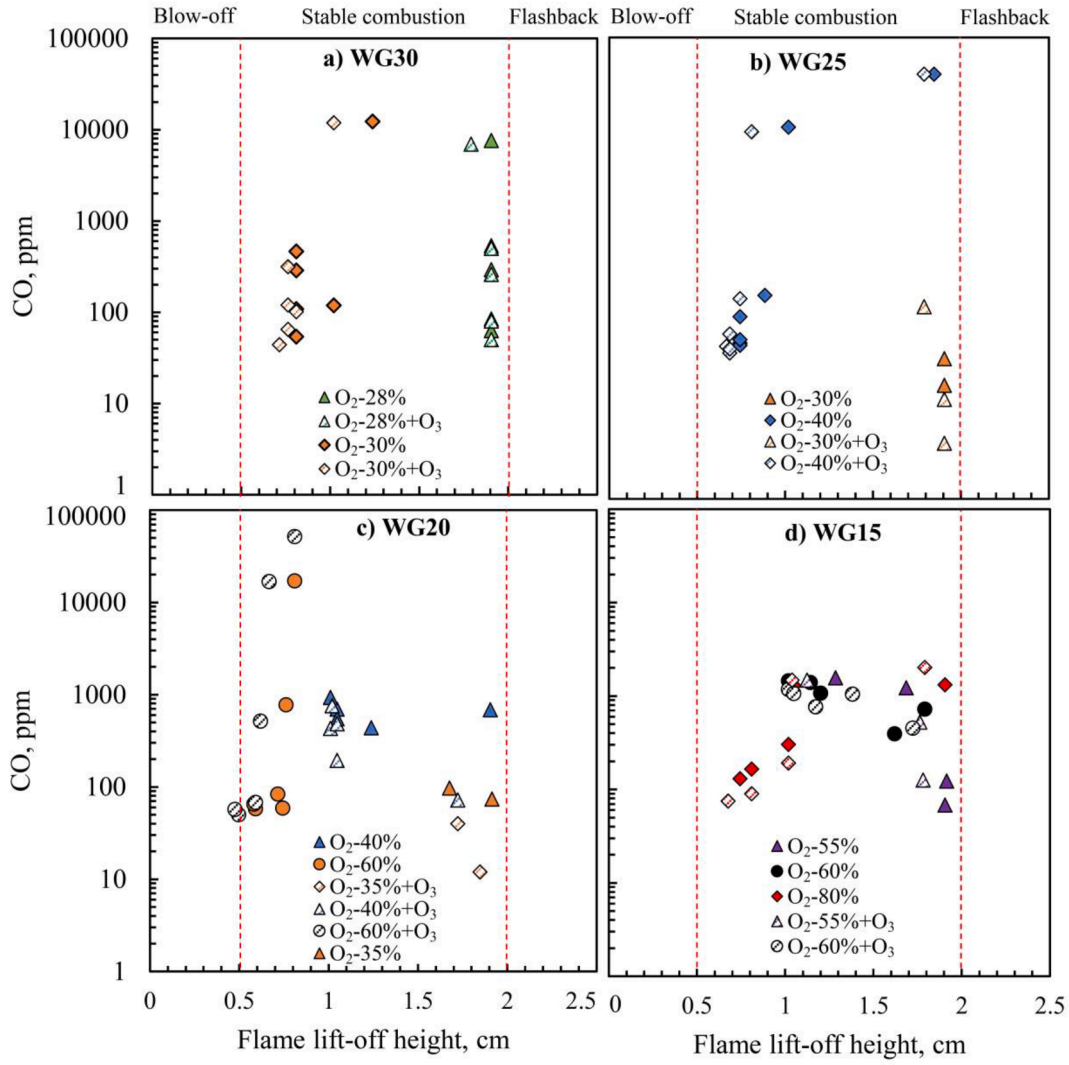

Fig. 5. CO emissions under different combustion conditions versus flame lift-off height.

values. Changing ϕ from 0.67 to 0.63, CO emissions decreased from 288 and 463 ppm to 120 and 314 ppm, but NOx emissions increased by 1–2 ppm, respectively (Fig. 5a and Fig. 6a). In the case of WG25 considerably small CO (up to 33 and 49 ppm) and NOx (up to 15 and 38 ppm) emissions were obtained at ϕ = 0.77–67 at both oxygen enrichment levels, respectively at 30 and 40 vol% (see Fig. 5b and Fig. 6b). During oxygen enrichment level of 40 vol%, the ϕ increase from 0.77 to 0.91 led to incomplete combustion and in increased CO emissions from 160 to 10674 ppm and flame lift-off height from 0.89 to 1.8 cm. Taking into account that the flame was lifted up and NOx emissions decreased by 15 ppm, it could be assumed that the flame temperature decreased at ϕ = 0.91. As in the previous case, the O_3 the highest reduction in CO (by 1186 ppm) was determined at ϕ = 0.91 under oxygen enrichment by 40 vol% (Fig. 5b), but NOx concentration increased by 1 ppm (Fig. 6b). At lower oxygen enrichment level (O_2–30 vol%), the enhancement by ozone led to reduced CO and NOx emissions respectively by 5–29 ppm and by 1–2 ppm changing ϕ from 0.77 to 0.71.

Similar results were determined during combustion of WG20 and WG15. The increasing oxygen enrichment level led to the flame position shift closer to the burner nozzle and more efficient combustion as CO emissions decreased. For instance, in the case of WG20 the increase of oxygen enrichment from 40 to 60 vol% led to decreased CO emissions from 350 to 868 ppm changing ϕ from 0.77 to 0.63 with the decrease of the flame lift-off (see Fig. 4c and Fig. 5c). At higher ϕ values, CO emissions increased drastically, up to 17000 ppm. However, considering the flame lift-off and NOx emissions, it could be assumed that the most efficient combustion of WG20 is achieved at oxygen enrichment of 40 vol%. Firstly, the flame is not attached close to the flashback or blowoff limit as in the case of O_2 enrichment by 35 vol% and NOx emissions are the lowest, (13–20 ppm at ϕ = 0.63–0.83) (Fig. 6c). It was determined that at O_2 enrichment by 80 vol% NOx emissions were higher by 12–15 ppm. Secondly, the ozone addition showed the highest influence on combustion enhancement in terms of the lift-off height and CO emission reductions. CO emissions were reduced by 612–64 ppm, but NOx emissions increased by 1–3 ppm changing ϕ from 0.91 to 0.66. Based on Fig. 6, the efficient combustion of WG15 was achieved under oxygen enrichment of 80 vol%. During combustion, CO emissions increased from 130 to 303 ppm changing ϕ from 0.63 to 0.71. Compared to CO emissions under O_2 enrichment of 60 vol% and 55 vol%, these were higher respectively by1324 ppm and by 1441–1065 ppm (Fig. 5d). But at higher ϕ values (0.77 – 0.83) incomplete combustion occurred and CO emissions increased up to ~1300 ppm and were higher by about 900 – 600 ppm compared to the case under oxygen enrichment of 60 vol%. Moreover, the flame position shifted up (Fig. 4d). Despite that, NOx emissions were low, up to 11 ppm, and similar in all cases (Fig. 6d). Regarding to [46], the high concentration of CO_2 in the mixture which in turn negatively affects the flame temperature and reduced N_2 concentration in the oxidizer leads to decreased rates of the Zel'dovich

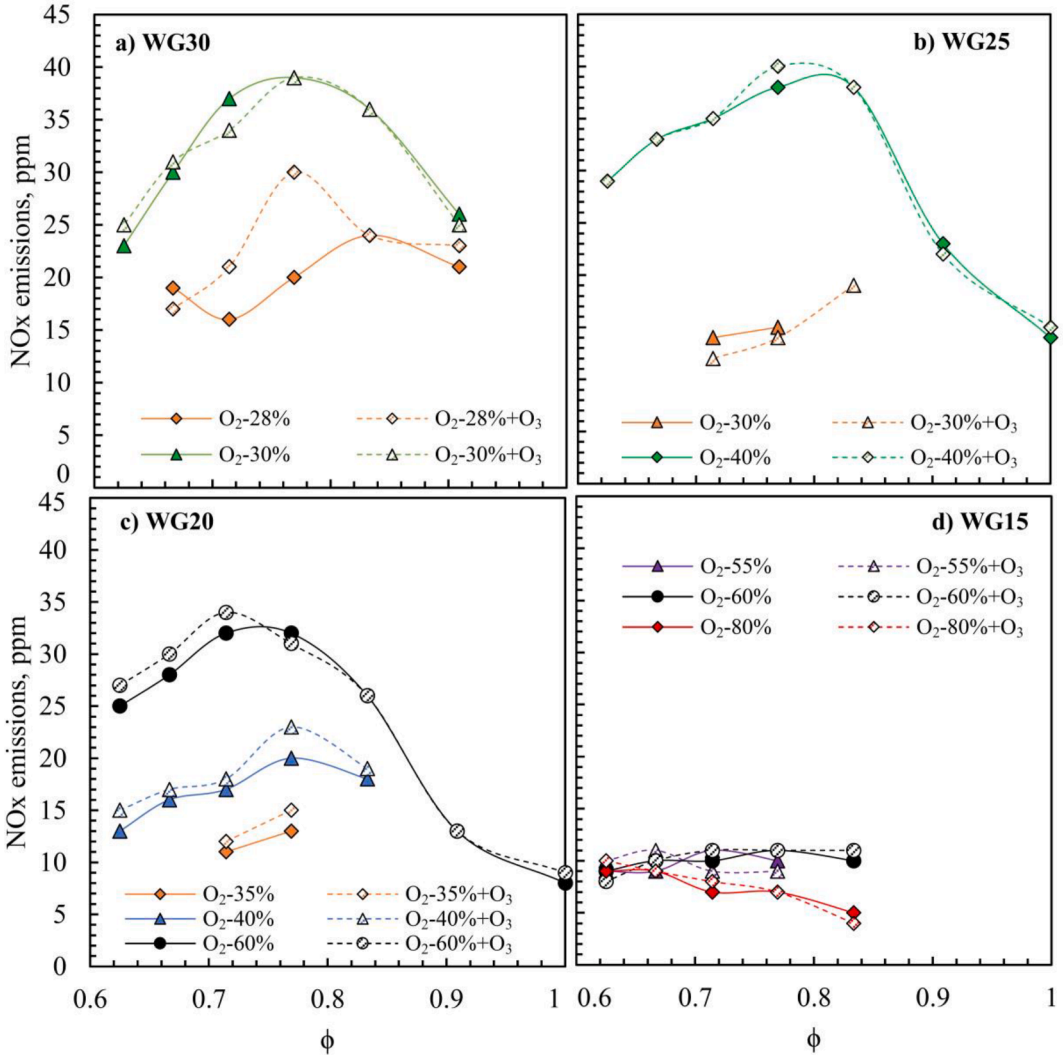

Fig. 6. NO_x emissions at different oxygen enrichment levels and fuel-air equivalence ratio ϕ.

reactions and reduced NOx emissions. Speaking of ozone effect on CO emissions in the case of WG15 under oxygen enrichment by 80 vol%, the CO reduction by the ozone addition was determined only at ϕ from 0.63 till 0.71 and CO emissions were reduced from 112 to 55 ppm, respectively. (Fig. 6d). Shifting ϕ from 0.71 to 0.83, the CO emissions increased drastically by 15–55% due to ozone addition. Based on the flame lift-off heights (Fig. 4d), changes of CO emissions correspond to the movement of the flame position and the increase in CO emissions occurs near the blowoff limit (see Fig. 5d). According to previous works [34,45] the increase of CO could be related to the decreased flow velocity caused by high oxygen concentration in the oxidizer. It leads to weaker mixing of reactants and incomplete combustion is intensified as the flame speed due to ozone addition increase.

4. Conclusions

The combustion enhancement of various waste gas mixtures (30–15 vol% of CH_4 in CO_2) by oxygen and ozone addition was investigated in the low swirl burner in lean-fuel conditions. Flame characteristics and performance under oxygen and ozone enrichment were determined using the flame emission spectroscopy method by registering chemiluminescent radical species OH*, CH* and C_2*, and using the flue gas analyser for post combustion products, namely CO and NOx, analysis, respectively. As a result, the following conclusions are made:

- The combustion of CH_4/CO_2 mixtures under oxygen enriched conditions showed that with the decreased methane concentration (from 30 to 15 vol%) in CO_2, the higher O_2 enrichment level (from 40 to 80 vol%) is required to achieve stable and efficient combustion process, but at higher oxygen enrichment levels, the flame is approaching to the flashback limit.
- The ozone addition leads to increased emission intensities of main radicals and greater effect of ozone is achieved for these flames which are lifted. This effect weakens with increasing oxygen enrichment level as the flame gets closer to the burner nozzle and flame stability is improved. It also corresponds to the flame lift-off reduction. During combustion of WG30 and WG25, the flame lift-off reduction (from 6.3 to 25.9% and from 8.3 to 25.9% respectively) by ozone intensified as the flame lift-off increased changing ϕ from 0.63 to 0.91. At lower methane concentrations, higher oxygen enrichment level leads to more attached flame to the burner nozzle and the ozone effect weakens. The WG15 flame lift-off height was reduced by 20.8–7% and by 10–3.7% at oxygen enrichment levels of 55 vol% and 60 vol%, while the lowest reduction (by 9–0.9% changing ϕ from 0.63 to 0.83) was determined at the oxygen enrichment level of 80 vol%.
- The combustion enhancement by ozone is closely related to calorific value in terms of methane concentration in the mixture and depends on the flame position as the highest effect of ozone in terms of reduced CO emissions and the flame lift-height was observed at

combustion conditions between blowoff and flashback limits. With occurrence of incomplete combustion of waste gases, CO emissions increase, and the flame is lifted and vice versa. In the case of WG30, significant effect of ozone was determined when flame is lifted. Changing ϕ from 0.67 to 0.63, CO emissions decreased from 288 and 463 ppm to 120 and 314 ppm, respectively. Meanwhile, the highest influence on combustion enhancement in terms of the lift-off height and CO emission reductions was determined for WG20. CO emissions were reduced by 612–64 ppm, but NOx emissions increased by 1–3 ppm changing ϕ from 0.91 to 0.66.

- The NOx emissions were not higher than 45 ppm (110 mg/m^3) under oxygen and ozone enriched conditions. Moreover, the NOx emissions decreased with decreasing CH_4 concentration in the mixture but increased with the increasing O_2 enrichment level due to increased flame temperature. Also, the plasma-produced ozone allowed to avoid the undesired plasma products, which occurs during plasma-assisted combustion and intensify NOx formation by 10 or more times. In this case, the addition of ozone showed an advantage as NOx emissions increased only up to 10 ppm (WG30), besides increasing oxygen enrichment resulted in the increase of NOx emission by small part (2–5 ppm) as nitrogen concentration in the oxidizer was reduced.
- Considering the combustion efficiency in terms of flame stability and CO emissions, the most efficient combustion of waste gases WG25 and WG20 was achieved respectively under oxygen enrichment of 40 vol% with addition of ozone at lean-fuel conditions (ϕ from 0.63 till 0.83).

Declaration of Competing Interest

The authors declare that they have no known competing financial interests or personal relationships that could have appeared to influence the work reported in this paper.

References

[1] Directorate-General for Climate Action (European Commission)Al C. Going climate-neutral by 2050. 2019. https://doi.org/10.2834/508867.

[2] Prussi M, Julea A, Lonza L, Thiel C. Biomethane as alternative fuel for the EU road sector: analysis of existing and planned infrastructure. Energy Strateg Rev 2021;33:100612. https://doi.org/10.1016/j.esr.2020.100612.

[3] González-Castaño M, Kour MH, González-Arias J, Baena-Moreno FM, Arellano-Garcia H. Promoting bioeconomy routes: From food waste to green biomethane. A profitability analysis based on a real case study in eastern Germany. J Environ Manage 2021;300:113788. https://doi.org/10.1016/j.jenvman.2021.113788.

[4] Riggio V, Comino E, Rosso M. Energy production from anaerobic co-digestion processing of cow slurry, olive pomace and apple pulp. Renew Energy 2015;83:1043–9. https://doi.org/10.1016/j.renene.2015.05.056.

[5] Mao C, Feng Y, Wang X, Ren G. Review on research achievements of biogas from anaerobic digestion. Renew Sustain Energy Rev 2015;45:540–55. https://doi.org/10.1016/j.rser.2015.02.032.

[6] Ardolino F, Cardamone GF, Parrillo F, Arena U. Biogas-to-biomethane upgrading: A comparative review and assessment in a life cycle perspective. Renew Sustain Energy Rev 2021;139:110588. https://doi.org/10.1016/j.rser.2020.110588.

[7] Ullah Khan I, Hafiz Dzarfan Othman M, Hashim H, Matsuura T, Ismail AF, Rezaei-DashtArzhandi M, et al. Biogas as a renewable energy fuel – A review of biogas upgrading, utilisation and storage. Energy Convers Manag 2017;150:277–94. https://doi.org/10.1016/j.enconman.2017.08.035.

[8] Kim GT, Seo BH, Lee WJ, Park J, Kim MK, Lee SM. Effects of applying non-thermal plasma on combustion stability and emissions of NOx and CO in a model gas turbine combustor. Fuel 2017;194:321–8. https://doi.org/10.1016/J.FUEL.2017.01.033.

[9] De Giorgi MG, Ficarella A, Sciolti A, Pescini E, Campilongo S, Di Lecce G. Improvement of lean flame stability of inverse methane/air diffusion flame by using coaxial dielectric plasma discharge actuators. Energy 2017;126:689–706. https://doi.org/10.1016/J.ENERGY.2017.03.048.

[10] Paulauskas R, Martuzevičius D, Patel RB, Pelders JEH, Nijdam S, Dam NJ, et al. Biogas combustion with various oxidizers in a nanosecond DBD microplasma burner. Exp Therm Fluid Sci 2020;118:110166. https://doi.org/10.1016/j.expthermflusci.2020.110166.

[11] Bak MS, Im S-K, Mungal MG, Cappelli MA. Studies on the stability limit extension of premixed and jet diffusion flames of methane, ethane, and propane using nanosecond repetitive pulsed discharge plasmas. Combust Flame 2013;160(11):2396–403. https://doi.org/10.1016/j.combustflame.2013.05.023.

[12] Li T, Adamovich IV, Sutton JA. Effects of non-equilibrium plasmas on low-pressure, premixed flames. Part 1: CH* chemiluminescence, temperature, and OH. Combust Flame 2016;165:50–67. https://doi.org/10.1016/J.COMBUSTFLAME.2015.09.030.

[13] Varella RA, Sagás JC, Martins CA. Effects of plasma assisted combustion on pollutant emissions of a premixed flame of natural gas and air. Fuel 2016;184:269–76. https://doi.org/10.1016/J.FUEL.2016.07.031.

[14] Yu Y, Li X, An X, Yu X, Fan R, Chen D, et al. Stabilization of a premixed methane-air flame with a high repetition nanosecond laser-induced plasma. Opt Laser Technol 2017;92:24–31. https://doi.org/10.1016/j.optlastec.2017.01.001.

[15] Liao Y-H, Zhao X-H. Plasma-Assisted Stabilization of Lifted Non-premixed Jet Flames. Energy Fuels 2018;32(3):3967–74. https://doi.org/10.1021/acs.energyfuels.7b03940.

[16] Barbosa S, Pilla G, Lacoste DA, Scouflaire P, Ducruix S, Laux CO, et al. Influence of nanosecond repetitively pulsed discharges on the stability of a swirled propane/air burner representative of an aeronautical combustor. Philos Trans R Soc A Math Phys Eng Sci 2015;373(2048):20140335. https://doi.org/10.1098/rsta.2014.0335.

[17] Elkholy A, Shoshyn Y, Nijdam S, van Oijen JA, van Veldhuizen EM, Ebert U, et al. Burning velocity measurement of lean methane-air flames in a new nanosecond DBD microplasma burner platform. Exp Therm Fluid Sci 2018;95:18–26. https://doi.org/10.1016/j.expthermflusci.2018.01.011.

[18] Bak MS, Do H, Mungal MG, Cappelli MA. Plasma-assisted stabilization of laminar premixed methane/air flames around the lean flammability limit. Combust Flame 2012;159(10):3128–37. https://doi.org/10.1016/j.combustflame.2012.03.023.

[19] Sagás JC, Maciel HS, Lacava PT. Effects of non-steady state discharge plasma on natural gas combustion: Flammability limits, flame behavior and hydrogen production. Fuel 2016;182:118–23. https://doi.org/10.1016/J.FUEL.2016.05.100.

[20] Mousavi SM, Kamali R, Sotoudeh F, Karimi N, Lee BJ. Numerical Investigation of the Plasma-Assisted MILD Combustion of a CH4/H2 Fuel Blend Under Various Working Conditions. J Energy Resour Technol 2021;143. https://doi.org/10.1115/1.4048507.

[21] Li M, Wang Z, Xu R, Zhang X, Chen Z, Wang Q. Advances in plasma-assisted ignition and combustion for combustors of aerospace engines. Aerosp Sci Technol 2021;117:106952. https://doi.org/10.1016/j.ast.2021.106952.

[22] Kim W, Snyder J, Cohen J. Plasma assisted combustor dynamics control. Proc Combust Inst 2015;35(3):3479–86. https://doi.org/10.1016/j.proci.2014.08.025.

[23] Kim GT, Yoo CS, Chung SH, Park J. Effects of non-thermal plasma on the lean blowout limits and CO/NOx emissions in swirl-stabilized turbulent lean-premixed flames of methane/air. Combust Flame 2020;212:403–14. https://doi.org/10.1016/j.combustflame.2019.11.024.

[24] Reuter CB, Ombrello TM. Flame enhancement of ethylene/methane mixtures by ozone addition. Proc Combust Inst 2021;38(2):2397–407. https://doi.org/10.1016/j.proci.2020.06.122.

[25] Zhang Y, Zhu M, Zhang Z, Shang R, Zhang D. Ozone effect on the flammability limit and near-limit combustion of syngas/air flames with N 2, CO 2, and H 2 O dilutions. Fuel 2016;186:414–21. https://doi.org/10.1016/j.fuel.2016.08.094.

[26] Ji S, Li Y, Tian G, Shu M, Jia G, He S, et al. Investigation of laminar combustion characteristics of ozonized methane-air mixture in a constant volume combustion bomb. Energy 2021;226:120349. https://doi.org/10.1016/j.energy.2021.120349.

[27] Choe J, Sun W. Blowoff hysteresis, flame morphology and the effect of plasma in a swirling flow. J Phys D Appl Phys 2018;51(36):365201. https://doi.org/10.1088/1361-6463/aad4dc.

[28] Li P, Li W, Wang K, Hu F, Ding C, Guo J, et al. Experiments and kinetic modeling of NO reburning by CH4 under high CO2 concentration in a jet-stirred reactor. Fuel 2020;270:117476. https://doi.org/10.1016/j.fuel.2020.117476.

[29] Yilmaz İ, Alabaş B, Taştan M, Tunç G. Effect of oxygen enrichment on the flame stability and emissions during biogas combustion: An experimental study. Fuel 2020;280:118703. https://doi.org/10.1016/j.fuel.2020.118703.

[30] Merlo N, Boushaki T, Chauveau C, de Persis S, Pillier L, Sarh B, et al. Experimental study of oxygen enrichment effects on turbulent non-premixed swirling flames. Energy Fuels 2013;27(10):6191–7. https://doi.org/10.1021/ef400843c.

[31] Li Bo, Shi B, Zhao X, Ma K, Xie D, Zhao D, et al. Oxy-fuel combustion of methane in a swirl tubular flame burner under various oxygen contents: Operation limits and combustion instability. Exp Therm Fluid Sci 2018;90:115–24. https://doi.org/10.1016/j.expthermflusci.2017.09.001.

[32] Ilbas M, Guler NU, Sahin M. Experimental and numerical investigation of biogas distributed combustion with different oxidizers in a swirl stabilized combustor. Fuel 2021;304:121452. https://doi.org/10.1016/j.fuel.2021.121452.

[33] Striūgas N, Zakarauskas K, Paulauskas R, Skvorčinskienė R. Chemiluminescence-based characterization of tail biogas combustion stability under syngas and oxygen-enriched conditions. Exp Therm Fluid Sci 2020;116:110133. https://doi.org/10.1016/j.expthermflusci.2020.110133.

[34] Skvorčinskienė R, Striūgas N, Zakarauskas K, Paulauskas R. Combustion of waste gas in a low-swirl burner under syngas and oxygen enrichment. Fuel 2021;298:120730. https://doi.org/10.1016/j.fuel.2021.120730.

[35] Carl SA, Van Poppel M, Peeters J. Identification of the CH + O2→ OH(A) + CO Reaction as the Source of OH(A-X) Chemiluminescence in C2H2/O/H/O2Atomic Flames and Determination of Its Absolute Rate Constant over the Range T = 296 to 511 K. J Phys Chem A 2003;107(50):11001–7. https://doi.org/10.1021/jp035568j.

[36] HARDALUPAS Y, ORAIN M. Local measurements of the time-dependent heat release rate and equivalence ratio using chemiluminescent emission from a flame. Combust Flame 2004;139(3):188–207. https://doi.org/10.1016/j.combustflame.2004.08.003.

[37] Wang ZH, Yang L, Li B, Li ZS, Sun ZW, Aldén M, et al. Investigation of combustion enhancement by ozone additive in CH4/air flames using direct laminar burning velocity measurements and kinetic simulations. Combust Flame 2012;159(1):120–9. https://doi.org/10.1016/j.combustflame.2011.06.017.
[38] Sun W, Gao X, Wu B, Ombrello T. The effect of ozone addition on combustion: Kinetics and dynamics. Prog Energy Combust Sci 2019;73:1–25. https://doi.org/10.1016/j.pecs.2019.02.002.
[39] Jiang C, Pan J, Yu H, Zhang Yi, Lu Q, Quaye EK. Effects of mixing ozone on combustion characteristics of premixed methane/oxygen in meso-scale channels. Fuel 2022;312:122792. https://doi.org/10.1016/j.fuel.2021.122792.
[40] Smith GP, Park C, Schneiderman J, Luque J. C2 Swan band laser-induced fluorescence and chemiluminescence in low-pressure hydrocarbon flames. Combust Flame 2005;141(1-2):66–77. https://doi.org/10.1016/j.combustflame.2004.12.010.
[41] Oh S, Park Y, Seon G, Hwang W, Do H. Impacts of N2 and CO2 diluent gas composition on flame emission spectroscopy for fuel concentration measurements in flames. Int J Heat Mass Transf 2020;149:119174. https://doi.org/10.1016/j.ijheatmasstransfer.2019.119174.
[42] European Parliament. Council of the European Union. Directive (EU) 2015/2193 of the European Parliament and of the Council on the limitation of emissions of certain pollutants into the air from medium combustion plants. vol. 451. 2014.
[43] Tachibana T, Hirata K, Nishida H, Osada H. Effect of ozone on combustion of compression ignition engines. Combust Flame 1991;85(3-4):515–9. https://doi.org/10.1016/0010-2180(91)90154-4.
[44] Wilk M, Magdziarz A. Ozone effects on the emissions of pollutants coming from natural gas combustion. Polish J Environ Stud 2010;19:1331–6.
[45] Striūgas N, Paulauskas R, Skvorčinskienė R, Lisauskas A. Investigation of waste biogas flame stability under oxygen or hydrogen-enriched conditions. Energies 2020;13(18):4760. https://doi.org/10.3390/en13184760.
[46] Miller JA, Bowman CT. Mechanism and modeling of nitrogen chemistry in combustion. Prog Energy Combust Sci 1989;15(4):287–338. https://doi.org/10.1016/0360-1285(89)90017-8.